DMD Fast Forward. Published on April 1, 2009 as doi:10.1124/dmd.109.027037

DMD #27037

BIOTRANSFORMATION OF AN $\alpha_4\beta_2$ NICOTINIC ACETYLCHOLINE RECEPTOR PARTIAL AGONIST IN SPRAGUE-DAWLEY RATS AND THE DISPOSITIONAL CHARACTERIZATION OF ITS *N*-CARBAMOYL GLUCURONIDE METABOLITE

Christopher L. Shaffer, Tim F. Ryder, Karthik Venkatakrishnan[1], Ilana K. Henne[2] and Thomas N. O'Connell

Departments of Pharmacokinetics, Pharmacodynamics and Metabolism (C.L.S., T.F.R., K.V., I.K.H.) and Exploratory Medicinal Sciences (T.N.O.), Pfizer Global Research and Development, Groton/New London Laboratories, Pfizer Inc., Groton, CT 06340

DMD Fast Forward. Published on April 1, 2009 as DOI: 10.1124/dmd.109.027037
This article has not been copyedited and formatted. The final version may differ from this version.

DMD #27037

Running Title: Characterization of an *N*-Carbamoyl Glucuronide Metabolite

Address correspondence to:

Dr. Christopher L. Shaffer
Pharmacokinetics, Dynamics and Metabolism
Pfizer Global Research and Development
Groton/New London Laboratories
Pfizer Inc.
Eastern Point Road, MS 8220–4186
Groton, CT 06340
Tel. 860.441.3377
Fax 860.686.6532
Email: Christopher.L.Shaffer@pfizer.com

Text pages: 32
Tables: 5
Figures: 6
References: 30
Words in Abstract: 243
Words in Introduction: 299
Words in Discussion: 1441

Abbreviations: 1, (1*S*,5*R*)-2,3,4,5-Tetrahydro-7-(trifluoromethyl)-1,5-methano-1*H*-3-benzazepine hydrochloride; [^{14}C]**1**, (1*S*,5*R*)-2,3,4,5-Tetrahydro-7-(trifluoromethyl)-1,5-methano-1*H*-4[^{14}C]-3-benzazepine hydrochloride; **2**, (1*S*,5*R*)-2,3,4,5-Tetrahydro-7-(trifluoromethyl)-1,5-methano-4-oxo-1*H*-3-benzazepine; **3**, (1*S*,5*R*)-2,3,4,5-Tetrahydro-7-(trifluoromethyl)-1,5-methano-1*H*-3-benzazepine-3-carboxaldehyde; AUC, area under the concentration-time curve; BDC, bile duct-cannulated; CID, collision-induced dissociation; CL, total serum clearance; COSY, correlation spectroscopy; EHC, enterohepatic cycling; GFR, glomerular filtration rate; HMBC, heteronuclear multiple bond correlation; HPLC, high-performance liquid chromatography; HSQC, heteronuclear single quantum coherence; k_{el}, elimination rate constant; LC-MS/MS, liquid chromatography-tandem mass spectrometry; LC-MS-NMR, liquid chromatography-mass spectrometry-nuclear magnetic resonance; LLOQ, lower limit of quantification; LSC, liquid scintillation counting; MeCN, acetonitrile; MRM, multiple-reaction monitoring; mrp, multidrug resistance-associated protein; TOCSY, total correlation spectroscopy.

Abstract

The metabolism and disposition of (1*S*,5*R*)-2,3,4,5-tetrahydro-7-(trifluoromethyl)-1,5-methano-1*H*-3-benzazepine (**1**), an $\alpha_4\beta_2$ nicotinic acetylcholine receptor partial agonist, was determined in Sprague-Dawley rats following oral administration of [^{14}C]**1**. In intact animals, mass balance was achieved within 48 h, with five-times more radioactivity excreted in urine than in feces. Compound **1** underwent renal and metabolic clearance equally, and exhibited a very long half-life attributable to a secondary peak occurring 8 h post-dose in its serum concentration-time curve. In bile duct-cannulated (BDC) rats, mass balance was also achieved within 48 h with 73.7%, 23.4% and 5.5% of the dose detected in bile, urine and feces, respectively. Rats metabolized **1** by two primary routes: four-electron oxidation to either four amino acids or a lactam, and formation of an *N*-carbamoyl glucuronide (**M6**), which was only detected in bile. The presence of **M6** solely in bile and the double-humped serum concentration-time curve of **1** suggested the indirect enterohepatic cycling of **1** via **M6** following oral administration. To explore this mechanistic hypothesis further, intravenous studies were conducted with **1** in both intact and BDC rats to determine the extent of **1** undergoing indirect enterohepatic cycling via **M6**. When compared to the pharmacokinetics in intact rats, total serum clearance was higher (1.7-fold) and volume of distribution was lower (1.6-fold) in BDC rats, resulting in a correspondingly shorter (2.5-fold) half-life, with 56% of administered **1** undergoing recirculation, an amount consistent with that (68% of dose) of **M6** observed in bile from rats orally dosed [^{14}C]**1**.

Introduction

Enterohepatic cycling (EHC) is a distributional event in which a compound is absorbed from the intestine, excreted into bile and then reabsorbed into the portal vein following bile secretion into the intestine (Rowland and Tozer, 1995). This type of recirculation may occur to the administered compound directly and/or indirectly via its metabolite(s). For metabolite-mediated indirect EHC of a compound, one of the most common pathways is via a glucuronide conjugate (Scheline, 1973; Dickinson et al., 1979; Horton and Pollack, 1991; Bullingham et al., 1996; Skonberg et al., 2008). In these instances, the dosed compound (aglycone) experiences enzyme-mediated glucuronidation and the resulting glucuronide undergoes biliary clearance, ultimately entering the intestine upon bile secretion. Once in the intestinal lumen, the glucuronide is hydrolyzed, typically enzymatically (Scheline, 1973; Parkinson, 2001), to the aglycone, which reenters portal circulation. This process often results in a "double-humped" plasma concentration-time curve following oral dosing (Dickinson et al., 1979; Bullingham et al., 1996; Wajima et al., 2002), with the second peak arising from the originally ingested compound entering systemic circulation following its EHC causing increased exposure and a prolonged half-life.

Herein we report the absorption, metabolism and excretion of (1*S*,5*R*)-2,3,4,5-tetrahydro-7-(trifluoromethyl)-1,5-methano-1*H*-3-benzazepine (**1**), an $\alpha_4\beta_2$ nicotinic acetylcholine receptor partial agonist (Coe et al., 2005) potentially useful for smoking cessation, in Sprague-Dawley rats following a single oral dose of [^{14}C]**1** (Figure 1). During this radiolabeled mass balance study, specific phenomena were observed that suggested the enterohepatic recirculation of **1** via an *N*-carbamoyl glucuronide, its major

metabolite. To investigate this particular disposition further, a subsequent intravenous bolus study was conducted with **1** in both intact and BDC rats. A combination of the results from both the radiolabeled oral study and the non-radiolabeled intravenous pharmacokinetics study provided an integrated data set to define mechanistically the indirect EHC of **1** via its *N*-carbamoyl glucuronide in Sprague-Dawley rats.

Materials and Methods

Chemicals and Reagents. Compounds **1**, **2** (lactam metabolite) and **3** (formamide metabolite) were prepared by the Synthesis Group at Pfizer Global Research and Development (PGRD, Groton, CT); [^{14}C]**1** (52.0 mCi/mmol, 96.7% radiochemical purity, 98.5% enantiomeric excess) was synthesized by the Radiochemical Synthesis Group at PGRD (Groton, CT). The chemical purity of all synthetic compounds was >99%. Male Sprague-Dawley rat liver microsomes (RLMs; 21 mg protein/mL, 0.61 nmol P450/mg protein) were prepared by the Candidate Enhancement Group at PGRD (Groton, CT). β-Glucuronidase (EC 3.2.1.31, Type IX-A, 1–5×10^6 units/g protein) was obtained from Sigma Chemical Co. (St. Louis, MO). Jugular vein-cannulated/BDC male and female Sprague-Dawley rats were procured from Charles River Laboratories, Inc. (Wilmington, MA). Chemicals and solvents of reagent or HPLC grade were supplied by Aldrich Fine Chemical Co. (Milwaukee, WI), Fisher Scientific (Pittsburgh, PA) and the J.T.Baker Chemical Co. (Phillipsburg, NJ). Deuterated solvents were purchased from Cambridge Isotope Laboratories, Inc. (Cambridge, MA). All rat excreta, bile, sera and whole brains were collected gravimetrically and stored at –20 °C until analysis.

***In Vivo* Studies with [^{14}C]1.** The in-life portion of the study was conducted at Charles River Laboratories International, Inc. (Worcester, MA) in accordance with the Guide for the Care and Use of Laboratory Animals. Sprague-Dawley rats were fasted overnight prior to compound administration and for 2 h post-dose. A single dose (10 mg/kg, 40 μCi) of [^{14}C]**1** in deionized H_2O (5 mg/mL) was administered via oral gavage to each rat. Individual animal doses were calculated based on respective pre-treatment body weights and a dose volume of 2 mL/kg. The actual amount of dose solution

administered to each animal was determined by weighing the loaded dosing syringe before and after it was dispensed. The study included four groups of rats:

Group 1 (3/sex): From intact animals, urine and feces were collected separately into metabolism cage containers surrounded by dry ice pre-dose and in 24 h intervals from 0–168 h post-dose for the assessment of cumulative excretion of total radioactivity, mass balance and metabolite profiling and identification.

Group 2 (2/sex): From BDC animals, which received an infusion of a bile salts replacement solution (44 mmol cholic acid and 13 mmol $NaHCO_3$ per L 0.9% NaCl, pH 7.0–7.4) during the collection period, bile was collected into containers surrounded by cold packs pre-dose and from 0–4, 4–8, 8–12, 12–24 and 24–48 h post-dose for metabolite profiling and identification. Urine and feces were also collected from these animals in 24 h periods from 0–48 h post-dose.

Group 3 (3/sex): From jugular-vein cannulated rats, blood samples (0.5 mL) were collected just prior to dosing and at 0.25, 0.5, 1, 2, 4, 6, 8, 12 and 24 h post-dose for the pharmacokinetic evaluation of **1** and total radioactivity. After collection of the 1 and 8 h samples, whole blood (2 mL) from control donor animals was administered to each rat via the jugular vein cannula to maintain blood volume.

Group 4 (2/sex/time point): From intact animals, blood samples were collected by cardiac puncture following animal euthanasia by CO_2 asphyxiation at 1, 4, 8 and 24 h post-dose. Subsequently, the brain was extracted from each animal, rinsed of excess blood with saline, placed into a pre-weighed vial, weighed and snap frozen in liquid nitrogen.

All blood samples were collected into anticoagulant-free tubes and processed immediately to obtain serum. Control serum was harvested from blood collected from untreated animals that were not sacrificed.

Determination of Radioactivity within Biological Matrices. Triplicate gravimetric aliquots of each sample of urine (0.1 g), bile (0.05–0.1 g) and serum (0.05–0.1 g) were mixed with liquid scintillation cocktail (10 mL for bile, 5 mL for all other matrices) and counted for 2 min in a Model LS 6000 or LS 6500 liquid scintillation counter (Beckman Instruments, Richmond, CA).

Fecal samples were homogenized with deionized H_2O (20% w/w, feces/H_2O) using a probe-type homogenizer. Cage debris/rinse samples (collected in 50% reagent alcohol in H_2O) were homogenized directly with a probe-type homogenizer. Triplicate gravimetric aliquots (0.1–0.5 g for either fecal homogenate or cage debris/rinse homogenate) were transferred into tared cones and pads, weighed and combusted prior to radioanalysis. Sample combustion was performed using a Model 307 or 387 Sample Oxidizer (PerkinElmer Life Sciences, Inc., Boston, MA). Combustion efficiency using a [^{14}C]standard was determined daily prior to the combustion of study samples, and the measured radioactivity content in feces and cage debris/rinse was adjusted using daily combustion efficiency values. Liberated [^{14}C]CO_2 was trapped in Carbo-Sorb® E (Packard Instruments, Meriden, CT) and mixed with Permafluor E+ scintillation fluid (PerkinElmer Life Sciences, Inc.), and the samples were analyzed for total radioactivity in a Model LS 6000 or LS 6500 liquid scintillation counter (Beckman Coulter, Inc., Fullerton, CA) for 2 min. Scintillation counter data were automatically corrected for

counting efficiency using an external standardization technique and an instrument-stored quench curve generated from a series of sealed quench standards.

Thawed brains were weighed, diluted with H_2O (3 mL H_2O/g brain) and homogenized with a probe-type homogenizer. Following liquefaction, aliquots (0.2 g) of brain homogenate in scintillation cocktail (7 mL) were analyzed by LSC for 5 min.

Quantitative Analysis of 1 in Serum from Radiolabeled Studies. Serum concentrations of **1** were quantified using a characterized LC-MS/MS assay. To ensure that serum concentrations of **1** were within the dynamic range of the analytical assay, all samples, except the pre-dose samples, were diluted accordingly prior to analysis. To each serum aliquot (100 µL) contained in a 15 mL glass centrifuge tube was added 20% MeCN in H_2O (10 µL) containing an internal standard. Each sample was basified (100 µL, 0.1 M NaOH) and extracted with methyl *tert*-butyl ether (4 mL) via vortex-mixing and centrifugation (1,811 rcf for 10 min). The organic supernatant was transferred to a clean 15 mL glass centrifuge tube, concentrated to dryness under N_2 at 35 °C, and reconstituted in 20% MeCN in 10 mM ammonium formate, pH 3.0 (250 µL, Solvent A). Samples were analyzed by an LC-MS/MS comprised of a PE Sciex API-3000 tandem quadrupole mass spectrometer with a Turbo Ionspray® interface (PerkinElmer Life Sciences, Inc.), two Shimadzu LC-10A HPLC pumps (Shimadzu USA, Columbia, MD) and a CTC PAL Autosampler (LEAP Technologies, Carrboro, NC). Analytes within sample aliquots (20 µL) were eluted at 0.3 mL/min on a Phenomenex Synergi Max-RP analytical column (4 µ, 2.0×50 mm) using Solvent A and MeCN (Solvent B). The following one-step gradient was used: 0 to 4 min, 20% Solvent B in Solvent A; 4 to 5 min, 20% to 95% B in A; 5 to 7 min, 95% B in A. Following elution of **1** and the internal

standard, the column was returned over 1 min to 20% B in A where it remained for 4 min before the next injection. Mass spectral data were collected in positive ionization mode using MRM following the *m/z* 228.1→191.1 fragmentation for **1**. Instrument settings and potentials were adjusted to provide optimal data. The assay dynamic range was 0.25 to 50.0 ng/mL for **1**.

Pharmacokinetic Calculations for Radiolabeled Studies. Pharmacokinetic parameters were calculated for each rat by noncompartmental analyses using WinNonlin Professional Version 3.2 (Pharsight Corp., Mountain View, CA). Values used to determine the pharmacokinetic parameters of total radioactivity were calculated by converting the raw data generated by LSC to concentrations (ng-eq./mL) using the specific activity (3.6 mCi/mmol) of administered [^{14}C]**1**. The $AUC_{0–24}$ was calculated using the linear trapezoidal method, k_{el} was determined by linear regression of the log concentration versus time data during the last observable elimination phase, half-life ($t_{1/2}$) was calculated as $0.693/k_{el}$ and $AUC_{0–\infty}$ was calculated as the sum of $AUC_{0–24}$ and $AUC_{24–\infty}$, which was determined by dividing the plasma concentration at 24 h post-dose by k_{el}. Both maximal serum concentration (C_{max}) and its first time of occurrence (T_{max}) were taken directly from the serum concentration versus time data. Means and standard deviations were calculated when half or greater of the values exceeded the LLOQ for **1** (0.25 ng/mL) or total radioactivity (2× background radioactivity, which equated to 48 ng-eq./mL). A value of 0 was used when a measured value was <LLOQ.

Sample Preparation for Metabolite Profiling and Identification. At each step during the sample preparation of all biological matrices, total radioactivity levels were determined by LSC for recovery calculations. Following preparation, all samples were

DMD Fast Forward. Published on April 1, 2009 as DOI: 10.1124/dmd.109.027037
This article has not been copyedited and formatted. The final version may differ from this version.

analyzed as described later by LC-MS/MS with radiometric detection. Pre-dose and blank samples served as controls for determining background radioactivity and endogenous, non-compound-related ions observed within respective matrices or their extracts by LC-MS/MS.

Urine. Urine samples from each rat collected from 0–72 h post-dose representing ≥93% of total urinary radioactivity were pooled proportional to the amount of urine in each sampling period. Pooled samples were centrifuged (1,811 rcf for 5 min) to remove particulate materials, and the resulting supernatants were analyzed directly.

Bile. Bile collected from 0–24 h post-dose representing >89% of total biliary radioactivity were pooled proportional to the amount of bile in each sampling period. Pooled samples were centrifuged (1,811 rcf for 5 min) to sediment particulate materials affording the analytical supernatant.

Feces. Fecal homogenates (ca. 1.0 to 7.7 g) from each rat collected from 0–96 h post-dose, representing ≥95% of total fecal radioactivity, were pooled proportional to the amount of feces in each sampling period. After mixing at 37 °C for 14 h in a reciprocal water bath, pooled fecal homogenates were diluted with MeCN (3 mL/g homogenate), vortex-mixed and centrifuged (1,811 rcf for 10 min), and the resulting supernatants were isolated. If necessary, the remaining fecal pellets were extracted further with 33% H_2O in MeCN (6 mL) until ≥90% of the radioactivity, as determined by LSC analysis of the combined supernatants, from each pooled sample was extracted. The supernatants were concentrated to dryness by a N_2 stream at 35 °C and reconstituted in 10% MeCN in 10 mM ammonium formate, pH 3.4 (1 mL) for analysis.

Serum. Serum from blood samples collected by terminal bleeding of rats at 1, 4, 8 and 24 h post-dose were used for circulatory metabolite profiling and identification. Serum samples were pooled within gender according to the method of Hamilton *et al.* (Hamilton et al., 1981); i.e. 1.0, 1.8, 5.0 and 4.0 mL, respectively, of serum from each time point sample were combined to afford 11.8 mL of pooled serum for each gender profile. Proteins were precipitated from the serum pools by the addition of MeCN (24 mL), and the samples were vortex-mixed and centrifuged (1,811 rcf for 10 min). The remaining serum protein pellets were extracted an additional time with MeCN (4 mL) to ensure that >90% of radioactivity, as determined by LSC analysis of the pooled supernatants, from each pooled serum sample was extracted. The combined supernatants were concentrated to dryness and the resulting residues were reconstituted in 10 mM ammonium formate, pH 3.4 (0.6 mL) and analyzed by LC-MS/MS. Quantitative analysis was achieved by isolating HPLC effluent by a fraction collector set at 30 s intervals, and each respective fraction was mixed with TruCount scintillation fluid (7 mL) and subjected to LSC for 5 min. Individual serum radiochromatograms were generated from respective liquid scintillation data using Microsoft Excel® (Microsoft Office 2000® 9.0.7619 SP-3).

Brain. Thawed brains (2/time point/gender), isolated from the same rats sacrificed at 1, 4, 8 and 24 h post-dose for the collection of blood for circulatory metabolite profiling and identification, were weighed, diluted with H_2O (3 mL H_2O/g brain) and homogenized with a probe-type homogenizer. Brain homogenates were pooled within gender according to the method of Hamilton *et al.* (Hamilton et al., 1981); i.e. 1.0, 1.8, 5.0 and 4.0 g, respectively, of homogenate were combined from each time point sample, which

included 2 brains/gender. To precipitate proteins, the pooled homogenates (11.8 mL each) were diluted with MeCN (23.6 mL), vortex-mixed and centrifuged (1,811 rcf for 10 min). The protein sediments were not extracted further since >93% of radioactivity, as determined by LSC analysis of the supernatants, from each pooled sample was isolated by just one extraction. The supernatants were removed and concentrated to near dryness at 35 °C by a N_2 stream, and the resulting residues were reconstituted in 10% MeCN in 10 mM ammonium formate, pH 3.4 (1 mL) for analysis.

Metabolite Profiling, Identification and Quantification. Samples were analyzed by an LC-MS/MS (described previously) equipped with an Agilent Zorbax SB-C18 analytical column (5 μ, 4.6 × 150 mm) in series with a β-RAM radiometric detector (IN/US Systems, Inc., Tampa, FL) containing a liquid scintillant cell (500 μL). Analytes within sample aliquots (25–100 μL) were eluted at 1 mL/min with 10 mM ammonium formate, pH 3.4 (Solvent C) and MeCN (Solvent B). The following gradient was employed: 0–20 min, 10% Solvent B in Solvent C; 20–55 min, 10%–50% B in C; 55–58 min, 50%–80% B in C; 58–60 min, 80% C in B. Following the elution of **1** and its metabolites, the column was returned over 1 min to 10% B in C where it remained for 4 min prior to the next injection. Due to the coelution of two biliary metabolites (i.e. **M5** and **M6**) using the aforementioned gradient, bile samples were injected a second time using the same gradient profile but substituting 10 mM ammonium acetate, pH 7.0 as Solvent C to achieve baseline resolution of **M5** and **M6**. For each matrix, >99% of the radioactivity injected onto the column eluted during the 65 min gradient programs. HPLC effluent was split 1:9 between the mass spectrometer and the radiometric flow detector; liquid scintillation cocktail flowed at 3 mL/min to the radiometric detector.

DMD Fast Forward. Published on April 1, 2009 as DOI: 10.1124/dmd.109.027037
This article has not been copyedited and formatted. The final version may differ from this version.

Mass spectral data were collected, using electrospray ionization in the positive ion mode, in full, precursor ion, neutral loss, product ion and MRM scanning modes. Instrument settings and potentials were adjusted optimally in each mode. Analyst® version 1.3 (PerkinElmer Life Sciences) and Laura version 3.1.3.39 (LabLogic Systems Limited, Sheffield, UK) software were used for the acquisition and processing of mass spectral and radiochromatographic data, respectively. Metabolites were quantified by peak integration within generated radiochromatograms.

***In Vitro* Generation of *N*-Carbamoyl Glucuronide M6** (Schaefer, 1992)**.** Incubations (2.5 mL) were performed in a capped, but vented 15 mL Erlenmeyer flask under a CO_2-saturated atmosphere at 37 °C in a shaking water bath. Each incubation contained male RLMs (2 mg of protein/mL 0.1 M $NaHCO_3$ buffer, pH 7.5), $MgCl_2$ (25 μmol), **1** (0.063 μmol), uridine 5'-diphosphoglucuronic acid trisodium salt (13 μmol), alamethicin (125 μg) and D-saccharolactone (12 μmol). After 2 h, the incubation was quenched with MeCN (2.5 mL), vortex-mixed and centrifuged (1,811 rcf for 5 min), and the resulting supernatant was concentrated and reconstituted in 20% H_2O in MeCN (200 μL) for LC-MS/MS analysis.

Isolation of [^{14}C]M6 from Bile and Its NMR Analysis. From the 0–4 h bile sample collected from one rat, [^{14}C]**M6** was isolated for NMR analysis by preparative HPLC using the aforementioned LC-MS/MS system equipped with a Chromolith SpeedRod (4.6 × 50 mm; Merck KGaA, Darmstadt, Germany) connected to a Chromolith Performance analytical column (4.6 × 100 mm). Three successive HPLC reversed phase separations were performed using three different solvent gradients and manual fraction collection of

DMD Fast Forward. Published on April 1, 2009 as DOI: 10.1124/dmd.109.027037
This article has not been copyedited and formatted. The final version may differ from this version.

column effluent. This entire isolation procedure, as well as the LC-MS-NMR analysis of **1** and partially purified [^{14}C]**M6**, are described within the Supplemental Data.

The highly purified and concentrated bile sample containing [^{14}C]**M6** (ca. 330 μg) in DMSO-d_6 was analyzed on a Bruker BioSpin 600 MHz Avance DRX Spectrophotometer equipped with a 2.5 mm broadband inverse probe. Proton chemical shifts are reported in ppm (δ) relative to tetramethylsilane as referenced from the shift of residual protons in DMSO-d_6 (2.49 ppm). ^{1}H, COSY and TOCSY spectra were obtained at 298 K using double presaturation of solvent NMR resonances. An HSQC spectrum was obtained at 298 K using WET suppression and an HMBC spectrum was obtained at 298 K. ^{1}H NMR spectra were also obtained at 298 K and 373 K.

Treatment of Purified [^{14}C]M5 with β-Glucuronidase. Rat bile extract HPLC effluent (0.2 mL, 113 nCi), composed of ca. 90% [^{14}C]**M5** (ca. 27 nmol) and 10% [^{14}C]**M6** (ca. 3 nmol) and obtained as a side product of the purification of [^{14}C]**M6** for NMR analysis (see Supplemental Data), was diluted to 0.5 mL with buffer (0.1 M KH_2PO_4, pH 7.4) or β-glucuronidase (1,000 units in 0.3 mL buffer) in a 15 mL glass conical tube open to air. The samples were briefly vortex-mixed, and then incubated at 37 °C for 45 h in a shaking water bath. Aliquots (100 μL) were removed from each vial after 0, 2, 22 and 45 h of incubation, quenched with MeCN (100 μL), diluted with H_2O (200 μL), vortex-mixed and analyzed directly (50 to 100 μL analytical aliquots) by LC-MS/MS with radiometric detection.

***In Vivo* Studies with Non-radiolabeled 1.** The in-life portion of the study was conducted at PGRD (Groton, CT) in accordance with the Guide for the Care and Use of Laboratory Animals. Sprague-Dawley rats were fasted overnight prior to compound

administration and for 7 h post-dose. A single intravenous bolus dose (0.2 mg/kg) of **1** in deionized H_2O (0.2 mg/mL) was delivered via a jugular vein catheter to each rat. Individual animal doses were calculated based on respective pre-treatment body weights and a dose volume of 1 mL/kg. The study included two groups of rats:

Group 1 (3/sex): From jugular vein-cannulated (intact) rats, blood samples (0.3 mL) were collected at 0.083, 0.17, 0.33, 0.5, 0.67, 1, 1.5, 2, 3, 4, 7, 10, 14, 24, 32, 48 and 72 h post-dose for the pharmacokinetic evaluation of **1**. Whole blood replacement (ca. 3 mL/rat) from donor rats was performed at 10 h post-dose to replace the approximate amount of blood loss during the study. Serial blood samples were collected in microtainer tubes and placed on ice until centrifugation (13,400 rcf for 10 min) to prepare serum. Serum samples were transferred to 1.2 mL polypropylene tubes and stored frozen at -20 °C until analysis. Urine was collected from the metabolic cages over the following time intervals: 0–7, 7–24, 24–48 and 48–72 h post-dose. The urine volume was measured at the end of each collection interval, transferred to a polypropylene tube, and stored at -20 °C until analysis.

Group 2 (3/sex): From jugular vein-cannulated/BDC rats, blood samples (0.3 mL) were collected at 0.083, 0.25, 0.75, 1.5, 3, 7, 10, 24, 32, 48 and 72 h post-dose for the pharmacokinetic evaluation of **1**. Serial blood samples were collected in red-capped Microtainer® Brand tubes (Becton Dickson, Franklin Lakes, NJ) and placed on ice until centrifugation (13,400 rcf for 10 min) to prepare serum. Serum samples were transferred to 1.2 mL polypropylene tubes and stored frozen at -20 °C until analysis. Urine was collected from the metabolic cages over the following time intervals: 0–10, 10–24, 24–48 and 48–72 h post-dose. The urine volume was measured at the end of each collection

interval, transferred to a 1.2 mL polypropylene tube, and stored at -20 °C until analysis. Bile was collected via the bile duct catheter over the same time intervals as urine collection, and stored as described for urine samples.

Quantitative Analysis of 1 in Serum, Urine and Bile from Non-radiolabeled Studies. Serum, urine and bile concentrations of **1** were quantified using the characterized LC-MS/MS assay formerly described with a dynamic range of 0.25 to 50.0 ng/mL for **1**. To ensure that serum concentrations of **1** were within the dynamic range of the analytical assay, all samples, except the pre-dose samples, were diluted accordingly prior to analysis. Serum work-up was the same as discussed previously. For urine and bile, to each sample aliquot (100 μL) contained in a 15 mL glass centrifuge tube was added both 20% MeCN in H_2O (10 μL) containing an internal standard and MeCN (2 mL). The diluted sample was vortex-mixed and centrifuged (600 rcf for 10 min). The organic supernatant (2 mL) was transferred to a clean 15 mL glass centrifuge tube, concentrated to dryness under N_2 at 35 °C, and reconstituted in 20% MeCN in Solvent A (200 μL). Sample analysis was identical to that already described.

Pharmacokinetic Calculations for Non-radiolabeled Studies. For intravenous studies with **1**, the estimated initial concentration ($C_{0(est)}$), area under the serum concentration-time curve from time 0 to the last measurable serum concentration ($AUC_{0-Tlast}$), $AUC_{0-\infty}$, k_{el}, $t_{1/2}$, total serum clearance (CL) and volume of distribution at steady-state (V_{ss}) were calculated from the serum concentration versus time data in individual animals by noncompartmental analysis as described beforehand. The cumulative percent of the dose recirculated was calculated as follows (Horton and Pollack, 1991), where

AUC_I and AUC_{BDC} are the mean $AUC_{0-\infty}$ values determined from intact (I) and BDC rats, respectively:

$$\text{Dose recirculated (\%)} = [(AUC_I - AUC_{BDC}) / AUC_{BDC}] \times 100$$

Renal clearance (CL_R) or biliary clearance (CL_{bil}) of **1** was calculated from the total amount of excreted **1** (A_e) detected within urine or bile, respectively, over 72 h and the serum $AUC_{0-\infty}$ of the intravenously dosed animals:

$$CL_R \text{ or } CL_{bil} \text{ (mL/min/kg)} = [A_e \text{ (ng)} / (AUC_{0-\infty} \text{ (ng•h/mL)} \times 60 \text{ (min/h)} \times BW \text{ (kg)})]$$

Results

Excretion of Total Radioactivity Following Oral Administration of [^{14}C]1. The excretion of total drug-related material was quite rapid in both genders; on average, >86% of the administered radioactivity was excreted within the first 48 h. Although there were no readily apparent gender-related differences in overall excretory routes or mass recoveries, male and female recovery values (mean ± SD) for both intact and BDC animals are listed in Table 1. Overall in intact rats, the mean recovery across genders of drug-related material within excreta and cage rinse was 101.2%±0.5%, with 84.2%±5.7% and 17.0%±6.1% of the dose detected within urine and feces, respectively. On average in BDC animals, 73.6%±22.4% of the dose was detected in bile from 0–48 h post-dose, with the 0–24 h bile sample comprising >89% of the 0–48 h biliary radioactivity (Table 1). Urine and feces collected from BDC animals over the 48 h interval accounted for on average across genders 23.3%±15.5% and 5.5%±7.3% of the administered dose, respectively.

Pharmacokinetics of 1 and Total Radioactivity Following Oral Administration of [^{14}C]1. As with total radioactivity excretion patterns, no obvious gender-related differences in systemic exposure to **1** or total radioactivity were observed. For **1**, its average serum concentration vs. time is plotted in Figure 2, and its gender-specific pharmacokinetic parameters (mean ± SD) are listed in Table 2. On average in males and females, serum concentrations of **1** rose to a mean C_{max} of 416±74 ng/mL at a mean T_{max} of 5.0±2.4 h post-dose with a mean $t_{1/2}$ of 16.2±5.5 h.

For total radioactivity, its average serum concentration-time curve and pharmacokinetic parameters (mean ± SD) are also in Figure 2 and Table 2, respectively.

On average in males and females, the mean C_{max} and T_{max} values of total radioactivity were 733±85 ng-eq./mL and 7.0±3.0 h, respectively, while the mean $t_{1/2}$ was 51.1±38.3 h. It is important to note that the reported elimination half-lives for both **1** and total radioactivity are considered estimates since the span ratio was less than two, and this has direct consequences on the degree of confidence in presented CL/*F* and AUC values, which also are estimates at best. On average in both genders, the $AUC_{0-\infty}$ for **1** represented 25.3% of the $AUC_{0-\infty}$ for total drug-related material. Interestingly, serum concentration-time curves for both **1** and total ^{14}C had a double-humped profile with the second upward leg occurring at ca. 6 h post-dose, suggestive of the EHC of **1**.

Structural Rationalization of 1 and Its Metabolites. Compound **1** had a protonated molecular ion of *m*/*z* 228 and an LC t_R of ca. 31.8 min. The CID product ion spectrum of *m*/*z* 228 contained fragment ions with *m*/*z* 211, 199, 196, 191, 179, 177, 159 and 141 (Table 3); structures for the majority of these fragment ions were mechanistically rationalized to facilitate metabolite structure elucidation (Figure 3). For metabolite identification purposes, precursor ion scanning of two diagnostic fragment ions *m*/*z* 191 (the base peak within the CID spectrum of **1**) and *m*/*z* 177 (a very minor ion within the CID spectrum of **1**) was undertaken. Fragmentation patterns of all detected metabolites and available metabolite synthetic standards (i.e. **2** and **3**) demonstrated that biotransformation on or directly adjacent to the nitrogen within **1** dramatically shifts the base peak of the modified compound from *m/z* 191 to *m/z* 177 due to a change in molecular electronics that alters the CID bond-breaking scenario proposed for **1** (Figure 3). Therefore, any metabolites detected by a precursor ion scan of *m/z* 191, but not *m/z* 177, would be predicted to be enzymatically modified in a region removed from the

alicyclic secondary nitrogen. A summary of all metabolite LC-MS/MS data is found in Table 3. Additionally, neutral loss of 176 scanning was used throughout MS analyses to detect specifically potential glucuronide metabolites. The identification of a metabolite as a fully characterized standard was determined by the compounds' indistinguishable CID spectra and LC t_Rs, as well as an increase in metabolite MS peak height upon addition of the authentic standard to the analytical sample.

A key interest of the metabolite identification work was the characterization of the suspected *N*-*O*-glucuronide (**M5**) and *N*-carbamoyl glucuronide (**M6**) metabolites; particularly, the chemical fate of both **M5** and **M6** when treated with β-glucuronidase and the definitive structure elucidation of the major bile-specific metabolite **M6**. Treatment of bile extracts containing **M5** (*m/z* 420, LC t_R ca. 38.5 min) with β-glucuronidase resulted in its full conversion to a new single radioactive peak (LC t_R ca. 37.7 min). Mass spectral analysis of the new radioactive peak detected two compound-related ions: *m/z* 244, 16 amu greater than **1**, and *m/z* 242, which had an LC t_R and CID spectrum identical to putative nitrone **M7**. The compound-related molecule with *m/z* 244 is believed to be *N*-hydroxyl-**1**, which could itself be oxidized further, either *in vitro*, upon sample work-up and/or within the MS source (Huizing and Beckett, 1980; Lindeke, 1982), to **M7**, which was the only one of these two compounds detected *in vivo*. Based on the enzymatic hydrolysis of **M5** to a compound with *m/z* 244 (Miller et al., 2004), the fact that no carbon-hydroxylated metabolite of **1** was observed in any biological matrix, and the structural rationalization of each fragment ion observed in its CID product ion spectrum (especially the *m/z* 244 and 226 fragments, which are believed to correspond to *N*-hydroxyl-**1** and its dehydrated iminium, respectively), **M5** was tentatively identified as

DMD Fast Forward. Published on April 1, 2009 as DOI: 10.1124/dmd.109.027037
This article has not been copyedited and formatted. The final version may differ from this version.

an *N*-*O*-glucuronide of **1**. Dissimilarly, **M6** was converted quantitatively to **1** by β-glucuronidase paralleling the hydrolytic behavior of *N*-carbamoyl glucuronides (Tremaine et al., 1989; Schaefer, 1992; Shaffer et al., 2005). Furthermore, an *N*-carbamoyl glucuronide of **1** was generated *in vitro*; the CID spectra, whose fragmentation cascades mirrored those of known *N*-carbamoyl glucuronides (Shaffer et al., 2005; Schaefer, 2006; Suzuki and Kamimura, 2007), and LC t_Rs of the biosynthesized *N*-carbamoyl glucuronide and **M6** were identical. NMR analyses of **M6** purified from rat bile extracts unequivocally identified it as an *N*-carbamoyl glucuronide of **1**. Specifically, the HMBC spectrum indicated a long range correlation between the anomeric proton and the carbamate carbon. Additionally, in LC-MS-NMR experiments, the $[M+D]^+$ detected by mass spectrometry for **M6** in deuterated solvents was 5 amu greater than its $[M+H]^+$ in non-deuterated solvents, consistent with four exchangeable protons within **M6**. A summary of all ^{1}H NMR data with full spectral assignments for both **1** and **M6** are within the Supplemental Data.

Quantitative Profile of [^{14}C]1 and Its Metabolites in Excreta. *Urine.* In addition to **1**, five urinary metabolites were observed for both genders (Table 1). Four metabolites (**M1**, **M2**, **M3** and **M4**) were proposed to be amino acids while the fifth (**M5**) was tentatively identified as an *N*-*O*-glucuronide of **1**. The structural assignments of **M1**, **M2**, **M3** and **M4** as amino acids arose from both structural deciphering of ion fragments within their respective CID spectra and the quantitative base-catalyzed hydrolysis of an authentic standard of **2** (4 μM in 1 M NaOH, 42 h, 25 °C) to two compounds, with LC t_Rs and CID spectra identical to **M2** and **M4**, in a ratio of 1:14 based on total ion intensity peak height ratios. Heating the basic aqueous solution to 70 °C for another 1 h (or 24 h)

DMD Fast Forward. Published on April 1, 2009 as DOI: 10.1124/dmd.109.027037
This article has not been copyedited and formatted. The final version may differ from this version.

increased the ratio, presumably via epimerization, of **M2**:**M4** to 1:2, suggesting **M4** was both the kinetically and thermodynamically favored diastereomeric amino acid, and was consistent with the metabolite ratios observed *in vivo*. Identical chemical behavior occurred during the base-catalyzed hydrolysis of the other regioisomeric lactam to **M1** and **M3**. On average in urine, 55.2%±6.8% of the administered dose was unchanged **1**, which equated to a renal clearance of 3× GFR (Davies and Morris, 1993).

Feces. In addition to **1**, only the urinary amino acid metabolites (**M1**, **M2**, **M3** and **M4**) were also observed in male feces, with all but **M1** detected in female feces. On average in feces, 5.5%±2.1% of the administered dose was unchanged **1** (Table 1).

Bile. In both genders, two glucuronide metabolites (**M5** and **M6**) were detected in bile with **M6** corresponding on average to 68% of administered **1** (Table 1). A trace amount (<1%) of **1** was detected within male bile only.

Quantitative Profile of [^{14}C]1 and Its Metabolites in Serum and Brain. In addition to **1**, six radioactive peaks were identified in both male and female serum: amino acids **M1**, **M2**, **M3** and **M4**, *N*-*O*-glucuronide **M5**, nitrone **M7**, lactam **2** and formamide **3** (Table 4). On average in serum, **1** comprised 14.0% of total serum radioactivity while the two most significant circulatory metabolites **M3/M4** and **2** accounted for 21.1% and 14.7%, respectively. In both genders, **1** represented 93% of total radioactivity in brain accompanied by only minor amounts of **2** and **3**.

Pharmacokinetics of 1 in Intact and BDC Rats Following Intravenous Administration of 1. Upon completing the mass balance study with [^{14}C]**1**, an intravenous bolus pharmacokinetic study was undertaken with non-radiolabeled **1** in both intact and BDC Sprague-Dawley rats to assess quantitatively its extent of EHC. Gender-

specific and mean (male and female) pharmacokinetic parameters (mean ± SD) for this study are summarized in Table 5. No gender differences in intravenous pharmacokinetics were obvious in either intact or BDC rats, thus mean serum concentration-time curves are plotted (Figure 4) and combined datasets were used for the statistical analysis of pharmacokinetic parameters (Table 5).

When compared to the pharmacokinetics in intact rats, CL in BDC rats was higher (1.7×; t-test p-value <0.01) and V_{ss} lower (1.6×; t-test p-value <0.01) resulting in a correspondingly shorter (2.5×; t-test p-value <0.01) $t_{1/2}$. These results suggest that the disposition of **1** in rats involves EHC. The cumulative percentage of the intravenous dose of **1** undergoing recirculation in rats was calculated to be 56% based on mean $AUC_{0-\infty}$ in intact and BDC animals. The CL_R of **1** in BDC rats was similar to that determined in intact animals, with the changes in CL resulting from higher (2.4×; t-test p-value <0.01) non-renal CL (CL_{nr}). In BDC rats CL_{bil} accounted for only 0.52% of the CL of **1**. Therefore, biliary excretion of hepatic biotransformation product(s) of **1** and their back-conversion to **1** and its reabsorption in the intestine (rather than direct recycling of **1** via biliary secretion) is likely to be the predominant underlying mechanism of EHC of **1** in Sprague-Dawley rats. Due to the lack of a synthetic standard of **M6**, only qualitative analyses of bile collected from intravenous studies could be conducted to determine the presence of **M6** within these samples. Thus, aliquots (100 μL) from bile samples (0–10 h and 10–24 h collection interval samples) underwent the developed metabolite identification LC-MS/MS methodology (i.e. neutral loss, precursor ion, and product ion scanning modes) described previously and were determined to contain **M6**.

Discussion

No obvious gender-related differences were observed for the pharmacokinetics, excretion patterns or metabolic profiles in Sprague-Dawley rats following a 10 mg/kg oral dose of [^{14}C]**1**. On average in intact animals, 101% of administered radioactivity was recovered over the study period with 84.2% in urine and 17.0% in feces. In BDC rats, mass balance (105%) was achieved within 48 h post-dose with 73.7%, 23.4% and 5.5% of the dose detected in bile, urine and feces, respectively. A relatively short T_{max} and large amounts of radioactivity excreted in bile and urine from 0–24 h post-dose suggest [^{14}C]**1** was readily and substantially absorbed in rats. In intact animals, **1** underwent renal and metabolic clearance equally, and exhibited a very long $t_{1/2}$. It is important to note, however, that the reported elimination half-lives are considered estimates since the span ratio was less than two, and this has direct consequences on the degree of confidence in presented CL/*F* and AUC values, which too are at best estimates. Active renal secretion of **1** was observed as its unbound CL_R was 3-fold greater than GFR. An average brain-to-serum $AUC_{0–24}$ ratio of 28 suggests **1** has extensive brain penetration in rats, consistent with its physicochemical properties and it not being a multidrug resistance 1 P-glycoprotein substrate.

A schematic overview of the metabolism of **1** in Sprague-Dawley rats is presented in Figure 5. Qualitatively identical and quantitatively similar metabolite profiles for **1** in all biological matrices were observed in both genders. Based upon the identification of all major metabolites in excreta, bile, serum and brain, **1** undergoes two primary routes of metabolism within rats: chronological *N*-carbamoylation and glucuronidation to generate an *N*-carbamoyl glucuronide (**M6**), and four-electron oxidation to either four amino acids

(**M1**, **M2**, **M3** and **M4**) or a lactam (**2**). Minor biotransformation pathways of **1** were oxidation to a putative hydroxylamine to afford a nitrone (**M7**) or *N*-O-glucuronide (**M5**), and *N*-formylation (**3**). Interestingly, certain metabolites were only observed in specific matrices. For example, amino acid metabolites (**M1**, **M2**, **M3** and **M4**) were detected in urine, feces and serum; their absence in brain and high percentages of total circulating radioactivity with only minor urinary quantities are likely attributable to their low volumes of distribution as expected by their polar, zwitterionic nature. Alternatively, lactam **2** was only observed in serum and brain. Its presence in circulation but absence in excreta suggest the possibility that it may be hydrolyzed (possibly enzymatically within the kidney) to its corresponding amino acids **M2** and **M4** prior to excretion. Although an authentic standard of **2** was readily converted to **M2** (minor) and **M4** (major) under aqueous basic conditions, **2** was completely stable in both RLMs (over 1 h, ±NADPH) and rat hepatocytes (over 4 h). This was also true for an authentic standard of the regioisomeric lactam of **2**, which produced **M1** (minor) and **M3** (major) when treated with aqueous base.

The most intriguing metabolic pathway for **1** was its conversion to *N*-carbamoyl glucuronide **M6**, which was isolated for its structural confirmation by NMR analysis; NMR and MS spectra of *N*-carbamoyl glucuronides are well-characterized in the literature (Shaffer et al., 2005; Schaefer, 2006). Additionally, the stability of *N*-carbamoyl glucuronides in buffer (Thomas et al., 2008), urine (Elvin et al., 1980; Straub et al., 1988), plasma (Tremaine et al., 1989) and serum (Thomas et al., 2008) are also nicely documented. More interesting than purely the identification of **M6** as an *N*-carbamoyl glucuronide was its influence over the disposition of **1** (and total radioactivity)

DMD Fast Forward. Published on April 1, 2009 as DOI: 10.1124/dmd.109.027037
This article has not been copyedited and formatted. The final version may differ from this version.

in rats following an oral dose of [^{14}C]**1**. Preliminary mass balance study observations of ≥80% of administered radioactivity excreted in urine and **1** being the major urinary component (≥63%) suggested **1** was well-absorbed and underwent only moderate metabolism *in vivo*. This initial theory was supported by BDC animal data in which large amounts (≥65%) of orally-dosed radioactivity were observed in bile with a concomitant drop in urinary and fecal radioactivity. These excretion patterns coupled with the double-humped serum concentration-time curves suggested that **1** was likely undergoing direct EHC. However, metabolite profiling of biliary radioactivity provided a much different interpretation, in that the predominant (>95%) biliary radioactive component was **M6**, a metabolite not detected in any other biological matrix, and not **1** (<1%). Together, these data clearly pointed to the indirect EHC of **1** via **M6**.

To define this suspicion more definitively, intravenous studies were conducted with **1** in both intact and BDC Sprague-Dawley rats to determine empirically the extent of **1** undergoing indirect EHC via **M6**. When compared to the pharmacokinetics in intact rats, CL in BDC rats was higher (1.7-fold) and V_{ss} was lower (1.6-fold), resulting in a correspondingly shorter (2.5-fold) $t_{1/2}$. These results suggest that the disposition of **1** in rats involves EHC, with 56% of the intravenous dose of **1** undergoing recirculation, an amount consistent with that (68% of dose) of **M6** observed in bile from rats orally dosed [^{14}C]**1**. The CL_R of **1** in BDC rats was similar to that in intact animals, with the changes in CL resulting from a 2.4-fold higher CL_{nr}. Additionally, CL_{bil} accounted for only 0.5% of the net CL of **1** in BDC rats, again consistent with <1% of **1** detected in bile from the oral radiolabeled study. Therefore, biliary clearance of a hepatic biotransformation product (i.e. **M6**) of **1**, its back-conversion to **1** and the reabsorption of **1** in the intestine

(rather than direct recycling of **1** via biliary excretion) is proposed as the principal underlying mechanism of EHC of **1** in Sprague-Dawley rats.

Based on the reported data, a molecular mechanism rationalizing the EHC of **1** is proposed in Figure 6. Following oral dosing and absorption, **1** undergoes hepatic-mediated metabolic conversion to **M6**, which itself undergoes biliary clearance. Bile excretion into the upper gastrointestinal tract exposes **M6** to intestinal microflora rich in β-glucuronidase (Scheline, 1973; Parkinson, 2001), the enzyme responsible for the quantitative conversion of **M6** to **1** *in vitro*, resulting in glucuronide hydrolysis and spontaneous decarboxylation to **1**, which is predominately reabsorbed and ultimately enters systemic circulation (Figure 6A). (Hypothetically, **M6**, which was converted directly to **1** by strong aqueous base (1 N NaOH, pH 14), may also be hydrolyzed non-enzymatically within the intestine (pH 6.8). However, this seems less likely as **M6** was completely stable in buffer (pH 7.4) at 37 °C for 45 h consistent with other *N*-carbamoyl glucuronides (Thomas et al., 2008).) This circulatory reentry of **1** manifests in the secondary peak in its serum concentration-time curve. A combination of the intact and BDC radiolabeled study data suggest this EHC phenomenon occurs over a fairly short period of time, as total dosed biliary radioactivity crests within the first 4 h post-dose and then declines over the next 4 to 8 h (Figure 6B) as the serum concentration-time curves within intact animals show a second peak at ca. 8 h post-dose (Figure 6C), consistent with the timing of the drop in biliary radioactivity in BDC animals.

The suggestion that the conversion of **1** to **M6** is mainly (if not exclusively) metabolically-mediated hepatically arises from hepatocyte incubations conducted with [^{14}C]**1** in which 80% of **1** was metabolized to **M6** over 4 h. Over a 1 h period, RLMs

(±NADPH, 2 mg protein/mL, 10 μM **1**) failed to metabolize **1**, but they did convert **1** to **M6** (ca. 15% conversion at 25 μM) when optimized for *N*-carbamoyl glucuronidation. These results are supported by a recent dataset (Cerny et al., 2008) reporting that under similar conditions hepatic microsomes had a 25-fold greater relative rate than intestinal microsomes for the formation of an *N*-carbamoyl glucuronide of the structurally similar secondary alicyclic amine Lorcaserin.

It is worthy of note that two glucuronide metabolites were observed in rats: the predominant *N*-carbamoyl glucuronide (**M6**) and the minor *N*-*O*-glucuronide (**M5**). Whereas **M6** was only in bile, **M5** was observed in bile (minimally), serum and urine. This suggests that once formed hepatically **M6** undergoes exclusive biliary clearance. Alternatively, **M5** does not solely undergo biliary clearance, rather it reaches systemic circulation and is ultimately excreted renally. This yet-defined selectivity may be due to a glucuronide-centric hepatic transporter, such as the organic ion transporter mrp2 (Klaassen and Watkins III, 1984; Keppler and Arias, 1997; Seitz et al., 1998; Xiong et al., 2000; Westley et al., 2006), within the canalicular membrane that results in the preferential transport of **M6** over **M5** into bile. Conversely, it may be hypothesized that **M5** undergoes preferential (versus **M6**) transport into blood, such as that mediated by mrp3 (Soroka et al., 2001; Villaneuva et al., 2008). This mrp2 hypothesis is currently being investigated within our laboratory using either probenecid-treated wild-type rats or Wistar TR$^-$ rats lacking mrp2 (Jansen et al., 1985; Xiong et al., 2000).

DMD Fast Forward. Published on April 1, 2009 as DOI: 10.1124/dmd.109.027037
This article has not been copyedited and formatted. The final version may differ from this version.

Acknowledgments

The authors would like to acknowledge Dr. Klaas Schildknegt of the Radiosynthesis Group at PGRD, Groton, CT for the synthesis and purification of [^{14}C]**1**, Dr. Jotham Coe for providing **1**, Mr. Jason McKinley for synthesizing **2** and Mr. Nga Do for supplying **3**.

References

Bullingham R, Monroe S, Nicholls A and Hale M (1996) Pharmacokinetics and Bioavailability of Mycophenolate Mofetil in Healthy Human Subjects after Single-Dose Oral and Intravenous Administration. *Journal of Clinical Pharmacology* **36:**315-324.

Cerny MA, Palamar S, Chen W and Sadeque AJM (2008) Formation of *N*-Carbamoyl Glucuronide Metabolite of Lorcaserin. *Drug Metabolism Reviews* **40:**62.

Coe JW, Brooks PR, Wirtz MC, Bashore CG, Bianco KE, Vetelino MG, Arnold EP, Lebel LA, Fox CB, Tingley III FD, Schulz DW, Davis TI, Sands SB, Mansbach RS, Rollema H and O'Neill BT (2005) 3,5-Bicyclic aryl piperidines: A novel class of $\alpha_4\beta_2$ neuronal nicotinic receptor partial agonists for smoking cessation. *Bioorganic and Medicinal Letters* **15:**4889-4897.

Davies B and Morris T (1993) Physiological Parameters in Laboratory Animals and Humans. *Pharmaceutical Research* **10:**1093-1095.

Dickinson RG, Harland RC, Ilias AM, Rodgers RM, Kaufman SN, Lynn RK and Gerber N (1979) Disposition of Valproic Acid in the Rat: Dose-Dependent Metabolism, Distribution, Enterohepatic Recirculation and Choleretic Effect. *The Journal of Pharmacology and Experimental Therapeutics* **211:**583-595.

Elvin AT, Keenaghan JB, Byrnes EW, Tenthorey PA, McMaster PD, Takman BH, Lalka D, Manion CV, Baer DT, Wolshin EM, Meyer MB and Ronfeld RA (1980) Tocainide Conjugation in Humans: Novel Biotransformation Pathway for a Primary Amine. *Journal of Pharmaceutical Sciences* **69:**47-49.

Hamilton RA, Garnett WR and Kline BJ (1981) Determination of Mean Valproic Acid Serum Levels by Assay of a Single Pooled Sample. *Clinical Pharmacology and Therapeutics* **29:**408-413.

Horton TL and Pollack GM (1991) Enterohepatic Recirculation and Renal Metabolism of Morphine In the Rat. *Journal of Pharmaceutical Sciences* **80:**1147-1152.

Huizing G and Beckett AH (1980) Metabolism of Clebopride *In Vitro*. Identification of *N*-Oxidized Products. *Xenobiotica* **10:**593-602.

Jansen PLM, Peters WH and Lamers WH (1985) Hereditary Chronic Conjugated Hyperbilirubinemia in Mutant Rats Caused by Defective Hepatic Anion Transport. *Hepatology* **5:**573-579.

Keppler D and Arias IM (1997) Hepatic Canalicular Membrane. Introduction: Transport Across the Hepatocyte Canalicular Membrane. *FASEB* **11:**15-18.

Klaassen CD and Watkins III JB (1984) Mechanisms of Bile Formation, Hepatic Uptake, and Biliary Excretion. *Pharmacological Reviews* **36:**1-67.

Lindeke B (1982) The Non- and Postenzymatic Chemistry of *N*-Oxygenated Molecules. *Drug Metabolism Reviews* **13:**71-121.

Miller RR, Doss GA and Stearns RA (2004) Identification of a Hydroxylamine Glucuronide Metabolite of an Oral Hypoglycemic Agent. *Drug Metabolism and Disposition* **32:**178-185.

Parkinson A (2001) Biotransformation of Xenobiotics, in: *Casarett and Doul's Toxicology: The Basic Science of Poisons* (Klaassen CD ed), pp 133-224, McGraw-Hill, New York.

Rowland M and Tozer TN (1995) Elimination, in: *Clinical Pharmacokinetics: Concepts and Applications* (Balado D ed), pp 156-183, Lippincott Williams & Wilkins, Philadelphia, PA.

Schaefer WH (1992) Formation of a Carbamoyl Glucuronide Conjugate of Carvedilol *In Vitro* Using Dog and Rat Liver Microsomes. *Drug Metabolism and Disposition* **20:**130-133.

Schaefer WH (2006) Reaction of Primary and Secondary Amines to Form Carbamic Acid Glucuronides. *Current Drug Metabolism* **7:**873-881.

Scheline RR (1973) Metabolism of Foreign Compounds by Gastrointestinal Microorganisms. *Pharmacological Reviews* **25:**451-523.

Seitz S, Kretz-Rommel A, Elferink RPJO and Boelsterli UA (1998) Selective Protein Adduct Formation of Diclofenac Glucuronide Is Critically Dependent on the Rat Canalicular Conjugate Export Pump (Mrp2). *Chemical Research and Toxicology* **11:**513-519.

Shaffer CL, Gunduz M, O'Connell TN, Obach RS and Yee S (2005) Biotransformation of a $GABA_A$ Receptor Partial Agonist in Sprague-Dawley Rats and Cynomolgus Monkeys: Identification of Two Unique *N*-Carbamoyl Metabolites. *Drug Metabolism and Disposition* **33:**1688-1699.

Skonberg C, Olsen J, Madsen KG, Hansen SH and Grillo MP (2008) Metabolic Activation of Carboxylic Acids. *Expert Opinion in Drug Metabolism and Toxicology* **4:**425-438.

Soroka CJ, Lee JM, Azzaroli F and Boyer JL (2001) Cellular Localization and Up-regulation of Multidrug Resistence-Associated Protein 3 in Hepatocytes and Cholangiocytes During Obstructive Cholestasis in Rat Liver. *Hepatology* **33:**783-791.

Straub K, Davis M and Hwang B (1988) Benzazepine Metabolism Revisited: Evidence for the Formation of Novel Amine Conjugates. *Drug Metabolism and Disposition* **16:**359-366.

Suzuki K and Kamimura H (2007) Pharmacokinetics and Metabolism of an α,β-Blocker, Amosulalol Hydrochloride, in Mice: Biliary Excretion of Carbamoyl Glucuronide *Biol. Pharm. Bull.* **30:**1580-1585.

Tremaine LM, Stroh JG and Ronfeld RA (1989) Characterization of a Carbamic Acid Ester Glucuronide of the Secondary Amine Sertraline. *Drug Metabolism and Disposition* **17:**58-63.

Villaneuva SSM, Ruiz ML, Ghanem CI, Luquita MG, Catania VA and Mottino AD (2008) Hepatic Synthesis and Urinary Elimination of Acetaminophen Glucuronide are Exacerbated in Bile Duct-Ligated Rats. *Drug Metabolism and Disposition* **36:**475-480.

Wajima T, Yano Y and Oguma T (2002) A Pharmacokinetic Model for Analysis of Drug Disposition Profiles Undergoing Enterohepatic Circulation. *Journal of Pharmacy and Pharmacology* **54:**929-934.

Westley IS, Brogan LR, Morris RG, Evans AM and Sallustio BC (2006) Role of mrp2 in the Hepatic Disposition of Mycophenolic Acid and Its Glucuronide Metabolites: Effect of Cyclosporine. *Drug Metabolism and Disposition* **34:**261-266.

Xiong H, Turner KC, Ward ES, Jansen PLM and Brouwer KLR (2000) Altered Hepatobiliary Disposition of Acetaminophen Glucuronide in Isolated Perfused Livers from Multidrug Resistance-Associated Protein 2-Deficient TR^- Rats. *Journal of Pharmacology and Experimental Therapeutics* **295:**512-518.

Footnote

[1]K.V. current affiliation: Millennium Pharmaceuticals Inc., Department of Clinical Pharmacology, 40 Landsdowne Street, Cambridge, MA 02139.

[2]I.K.H. current affiliation: Gilead Sciences, Inc., Drug Safety and Evaluation, 333 Lakeside Drive, Foster City, CA 94404.

Legends for Figures

Figure 1. Chemical structure of [^{14}C]**1** (∗ denotes ^{14}C).

Figure 2. Semilogarithmic (top) and linear (bottom) plots of mean serum concentrations of **1** (solid symbols) and total radioactivity (open symbols) in female (♦) and male (▲) rats administered [^{14}C]**1** (10 mg/kg, PO).

Figure 3. Proposed structural assignments and fragmentation pathways for the CID spectrum of protonated **1** (*m/z* 228).

Figure 4. Semilogarithmic plot of mean serum concentrations of **1** in intact (■) and BDC (□) rats administered **1** (0.2 mg/kg, IV).

Figure 5. An overview of the proposed metabolic pathways of **1** in rats. Bold numerical designations are for observed metabolites; all other structures are putative metabolite intermediates.

Figure 6. The proposed mechanism for the EHC of **1** via **M6** (panel A), biliary radioactivity in female BDC rats over 24 h (panel B) and serum concentrations of **1** (♦) and total ^{14}C (◊) in female intact rats over 24 h (panel C).

Tables

Table 1. Cross-gender comparison of excretory routes and metabolite profiles (mean ± SD) following oral administration of [^{14}C]**1**

	Male[a]		Female[a]		Male[b]	Female[b]
Recovery[c]	102 ± 0		103 ± 0		111[d]	99.0[d]
	Urine	Feces	Urine	Feces	Bile	Bile
Dose excreted[c]	79.8 ± 2.7	21.6 ± 3.0	88.6 ± 3.9	12.3 ± 4.2	82.3	65.1
^{14}C profiled[e] (%)	85.0 ± 2.2	60.2 ± 1.3	87.0 ± 1.1	69.0 ± 1.3	98.4	95.5
	Metabolite Profile[c]					
1	50.3 ± 2.0	6.1 ± 1.3	60.1 ± 6.3	4.8 ± 2.8	0.8	—
M1	4.8 ± 0.7	0.9 ± 0.3	3.3 ± 0.9	—	—	—
M2	5.7 ± 1.1	2.1 ± 0.9	3.8 ± 0.7	1.5 ± 0.3	—	—
M3	2.1 ± 0.8	1.9 ± 0.2	5.1 ± 0.3	1.1 ± 0.2	—	—
M4	2.5 ± 0.6	1.9 ± 0.2	0.8 ± 0.7	1.1 ± 0.2	—	—
M5	2.6 ± 0.3	—	4.0 ± 1.2	—	3.2	2.4
M6	—	—	—	—	77.0	59.8
M7	—	—	—	—	—	—
2	—	—	—	—	—	—
3	—	—	—	—	—	—

—, not detected.
[a]Intact animals (Group 1, N=3/gender).
[b]Bile duct-cannulated animals (Group 2, N=2/gender).
[c]% of dose.
[d]Sum of dose recovered in bile, urine and feces from 0–48 h post-dose. In male bile duct-cannulated rats, 17.7% and 9.0% of the dose was excreted in urine and feces, respectively. For female counterparts, 29.0% and 2.0% of the dose was recovered in urine and feces, respectively.
[e]For each matrix, this value is calculated by dividing the sum of the metabolite profile by the total dose excreted and multiplying by 100.

DMD Fast Forward. Published on April 1, 2009 as DOI: 10.1124/dmd.109.027037
This article has not been copyedited and formatted. The final version may differ from this version.

Table 2. Cross-gender pharmacokinetics summary (mean ± SD) for **1** and total radioactivity following oral administration of [^{14}C]**1**

	1		Total Radioactivity	
	Male	Female	Male	Female
T_{max} (h)	6.7 ± 2.3	3.3 ± 1.2	8.0 ± 4.0	6.0 ± 2.0
C_{max}[a]	374 ± 71	459 ± 57	763 ± 104	704 ± 67
$t_{1/2}$ (h)	14.9 ± 2.8	17.5 ± 7.9	29.8 ± 15.7	72.4 ± 45.5
AUC_{0-24}[b]	5763 ± 506	7487 ± 649	13833 ± 751	14033 ± 1069
$AUC_{0-\infty}$[b]	8863 ± 1418	12967 ± 1582	33733 ± 13387	69600 ± 37532
CL/F[c]	16.9 ± 2.5	14.0 ± 1.9	na	na
CL_R[c,d]	8.45 ± 0.94	8.35 ± 0.49	na	na
$(CL_R/f_u)/GFR$[e]	3.1 ± 0.3	2.5 ± 0.2	na	na

na, not applicable.

[a]Units are ng/mL and ng-eq./mL for **1** and total radioactivity, respectively.

[b]Units are ng•h/mL and ng-eq.•h/mL for **1** and total radioactivity, respectively.

[c]Units are mL/min/kg.

[d]Calculated by $Ae_{0-168}/AUC_{0-\infty}$ and animal weight-normalized.

[e]Unbound plasma fraction was 0.60, GFR was assumed to be 1.31 mL/min (Davies and Morris, 1993) and animal weight-normalized.

DMD Fast Forward. Published on April 1, 2009 as DOI: 10.1124/dmd.109.027037
This article has not been copyedited and formatted. The final version may differ from this version.

Table 3. Chromatographic and mass spectral data for **1** and its metabolites

Compound	LC t_R (min)	$[M+H]^+$ (*m/z*)	CID-generated Fragments[a] (*m/z*)
1	31.8	228	211, 199, 196, **191**, 179, 177, 159, 141
M1	26.5	260	197, **177**, 159, 128
M2	27.3	260	197, **177**, 159, 128
M3	29.3	260	197, **177**, 159, 128
M4	29.7	260	197, **177**, 159, 128
M5	38.5/31.2[b]	420	244, **228**, 226, 197, 191, 177, 101, 83, 73
M6	38.5/32.8[b]	448	272, 252, 228, **177**, 165, 88
M7	38.0	242	224, 197, **177**, 128
2	41.8	242	213, 193, **177**, 165, 159, 144, 127
3	47.1	256	191, **177**, 142

[a]Bold font denotes base peak *m/z* within CID spectrum.

[b]LC t_R using 10 mM ammonium formate, pH 3.4 or 10 mM ammonium acetate, pH 7.0, respectively, as the aqueous mobile phase component.

DMD Fast Forward. Published on April 1, 2009 as DOI: 10.1124/dmd.109.027037
This article has not been copyedited and formatted. The final version may differ from this version.

Table 4. Cross-gender comparison of circulatory and brain metabolite profiles following oral administration of [^{14}C]**1**

	Male[a]		Female[a]	
	Serum	Brain	Serum	Brain
^{14}C Profiled (%)	80.3	100	75.2	100
	Metabolite Profile[b]			
1	12.4	93.1	15.5	93.2
M1/M2[c]	10.5	—	9.3	—
M3/M4[c]	26.0	—	16.2	—
M5	7.8	—	13.3	—
M6	—	—	—	—
M7	6.4	—	4.2	—
2	15.5	3.1	13.8	2.1
3	1.7	3.8	2.9	4.7

—, not detected.

[a]Intact animals (Group 4, N=2/gender/time point).

[b]% of total ^{14}C $AUC_{0–24}$.

[c]Metabolites were quantified as one radioactive entity since they were resolved by mass spectrometry, but not by radiochromatography.

DMD Fast Forward. Published on April 1, 2009 as DOI: 10.1124/dmd.109.027037
This article has not been copyedited and formatted. The final version may differ from this version.

Table 5. Cross-gender pharmacokinetics summary (mean ± SD) for **1** in intact and bile duct-cannulated (BDC) animals following an intravenous bolus of **1**

	Intact			BDC		
	Male	Female	Average	Male	Female	Average
CL[a]	27.5 ± 6.2	23.6 ± 3.1	25.6 ± 4.9	49.5 ± 8.6	34.2 ± 12.7	42.9 ± 12.5**
V_{ss} (L/kg)	18.4 ± 1.8	13.7 ± 2.1	16.0 ± 3.1	10.5 ± 0.8	8.95 ± 1.24	9.81 ± 1.22**
$t_{1/2}$ (h)	8.57 ± 1.84	7.02 ± 0.91	7.80 ± 1.55	2.85 ± 0.81	3.59 ± 0.99	3.17 ± 0.90**
$AUC_{0-Tlast}$[b]	119 ± 29	136 ± 17	127 ± 23	66.2 ± 15.5	101 ± 47	81.3 ± 34.9
$AUC_{0-\infty}$[b]	125 ± 29	143 ± 18	134 ± 24	69.3 ± 14.5	108 ± 46	86.1 ± 35.2
EHC[c]	80.4	32.4	55.6	na	na	na
CL_R[a,d]	12.4 ± 4.1	14.3 ± 1.5	13.3 ± 3.0	13.5 ± 2.4	13.2 ± 5.8	13.3 ± 3.8
CL_{nr}[a]	15.1 ± 3.0	9.33 ± 1.72	12.2 ± 3.8	36.0 ± 7.7	21.0 ± 7.4	29.6 ± 10.6**
CL_{bil}[a,d]	nd	nd	na	0.29 ± 0.18	0.14 ± 0.02	0.23 ± 0.15

na, not applicable; nd, not determined.

**Significantly different from the corresponding estimate in intact rats (t-test p value <0.01).

[a]Units are mL/min/kg.

[b]Units are ng•h/mL.

[c]% of dose undergoing enterohepatic cycling (EHC).

[d]Calculated by $Ae_{0-72}/AUC_{0-\infty}$ and animal weight-normalized.

DMD Fast Forward. Published on April 1, 2009 as DOI: 10.1124/dmd.109.027037

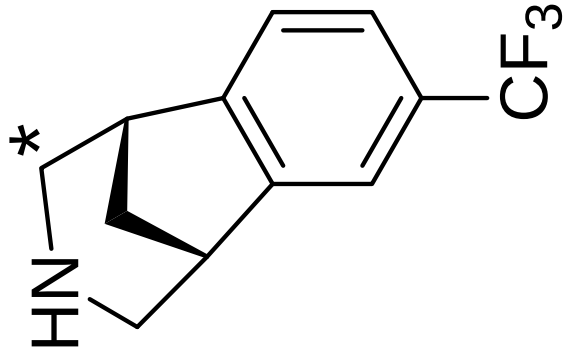

Figure 1

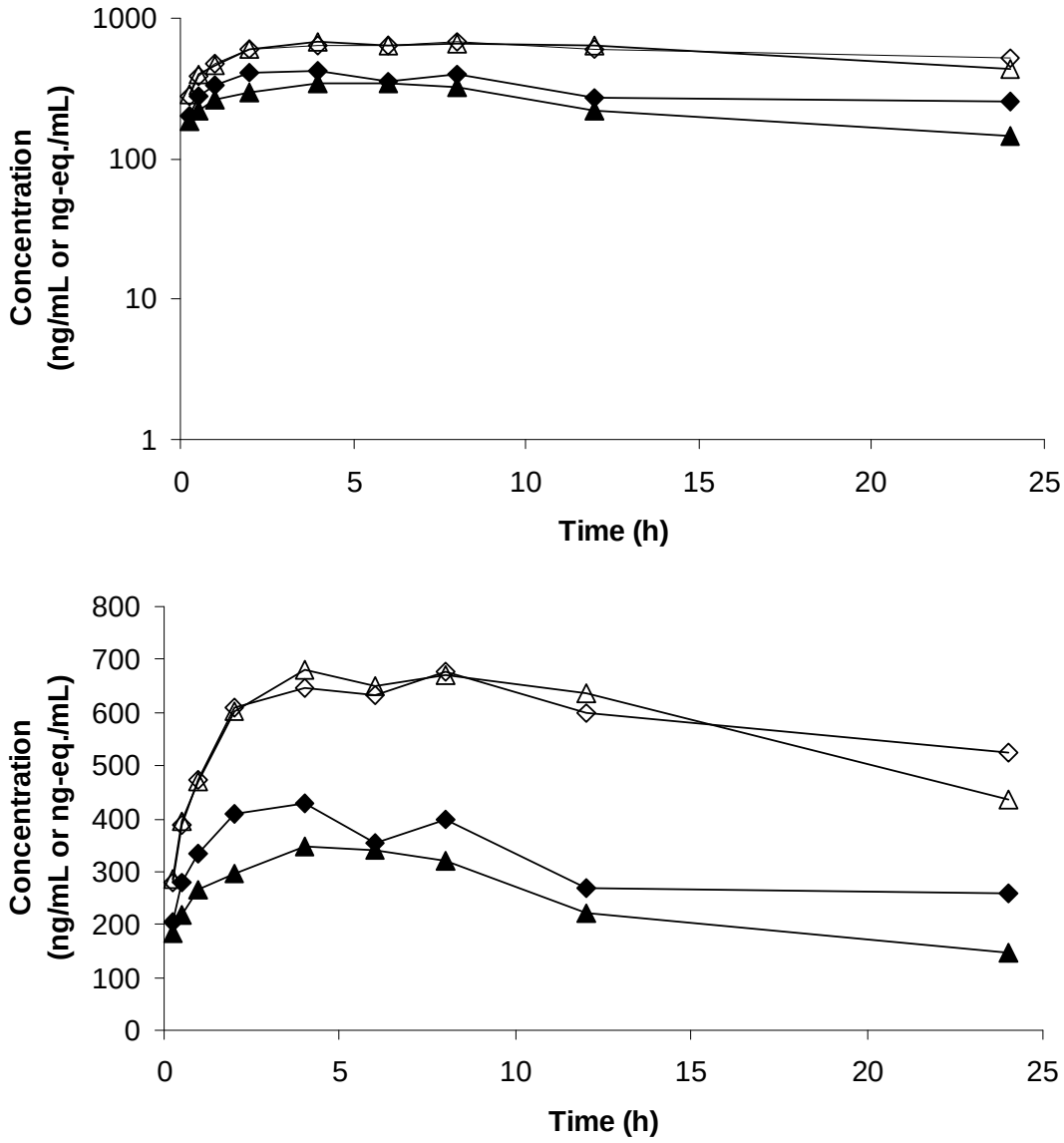

Figure 2

Figure 3

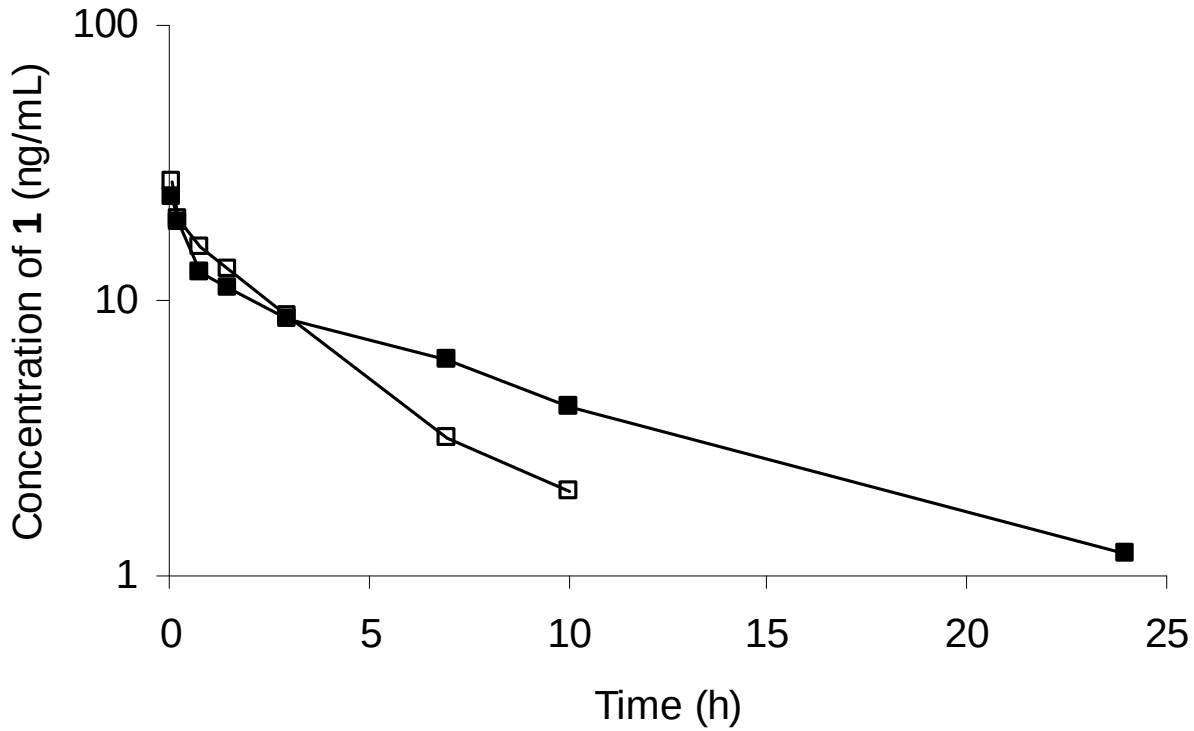

Figure 4

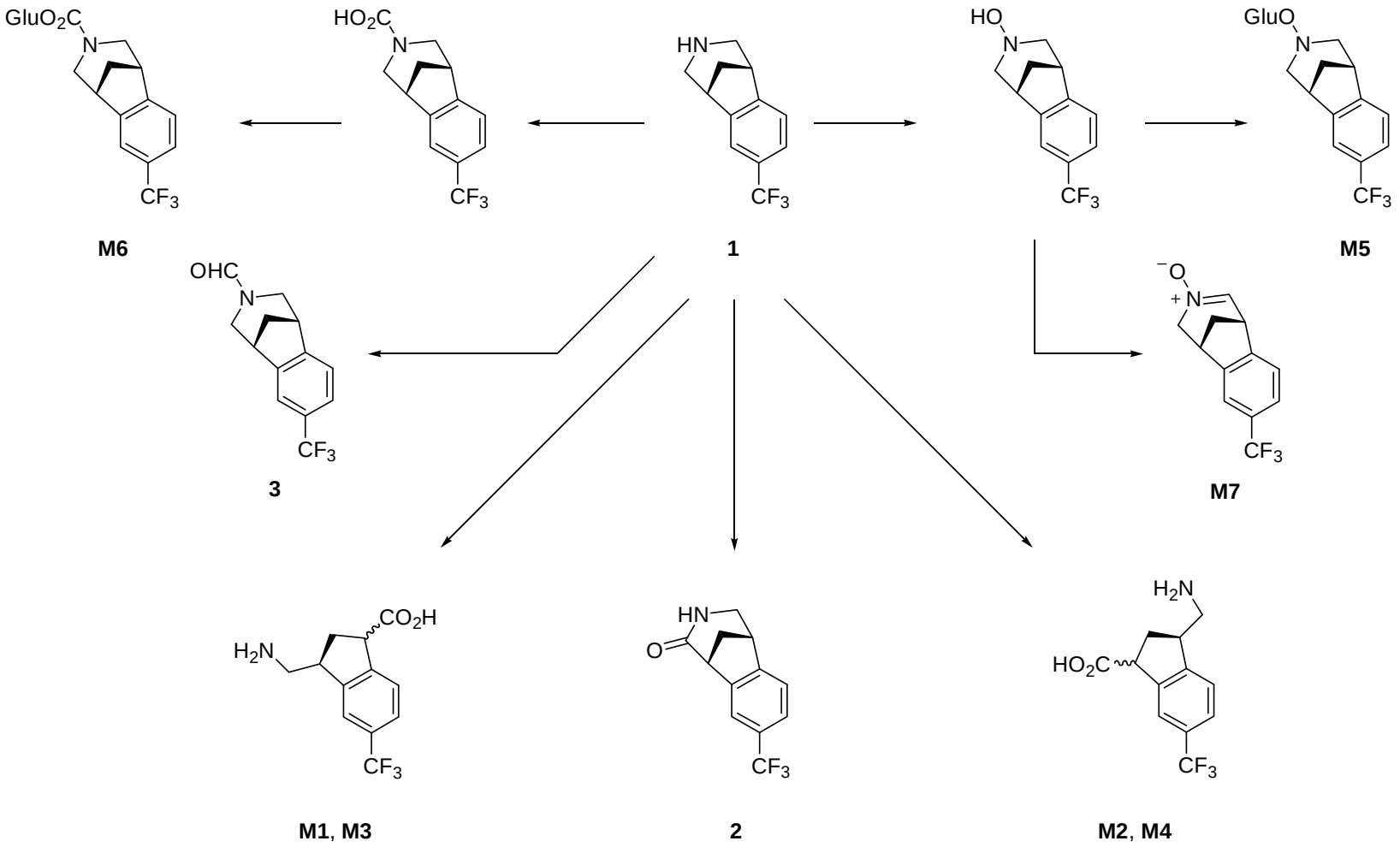

Figure 5

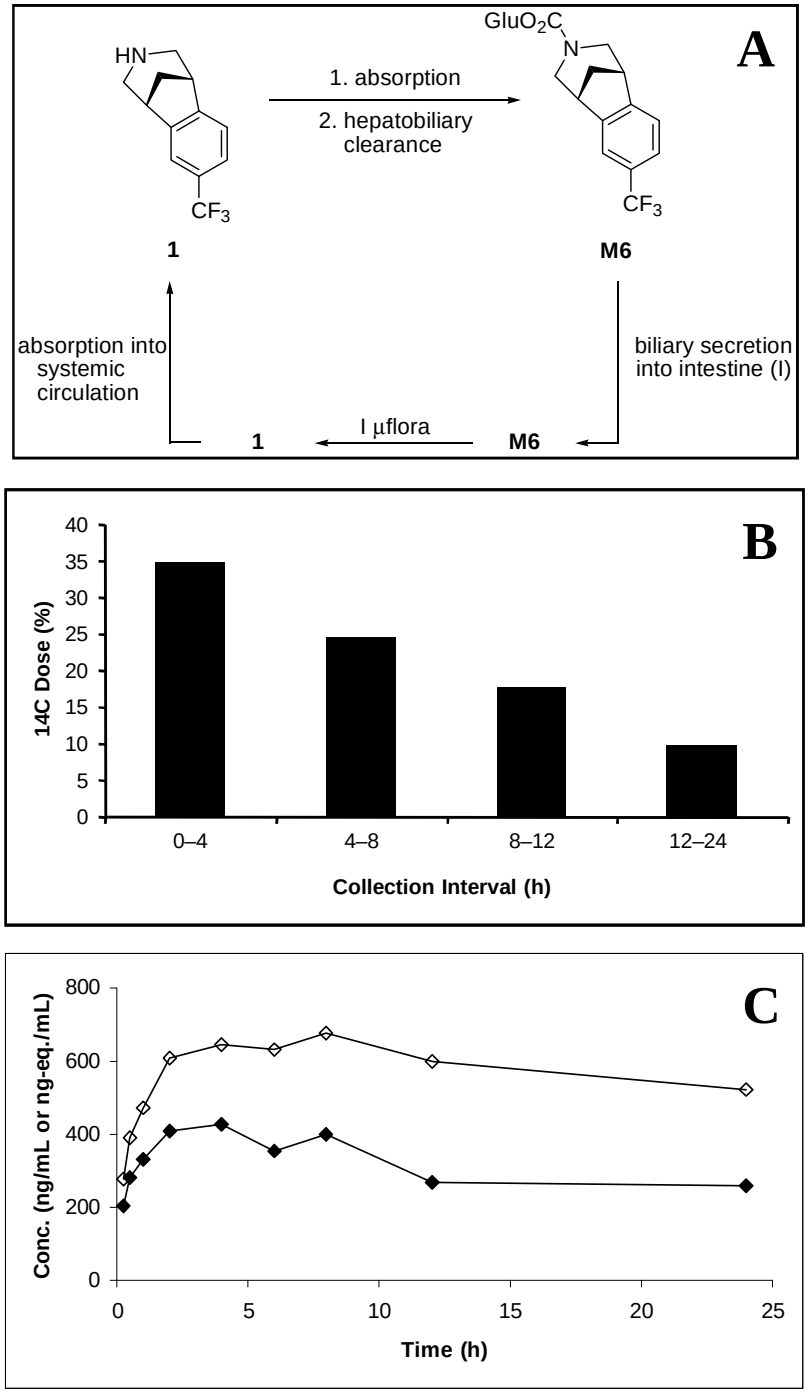

Figure 6